Published in final edited form as:
Amyloid. 2014 June ; 21(2): 103–109. doi:10.3109/13506129.2014.888994.

The critical role of the central hydrophobic core (residues 71-77) of amyloid-forming αA66-80 peptide in α-crystallin aggregation: A systematic proline replacement study

Rama Kannan[a], **Murugesan Raju**[b], and **K. Krishna Sharma**[a,b,*]

[a]Department of Biochemistry, University of Missouri, Columbia, Missouri 65211, United States

[b] Department of Ophthalmology, University of Missouri School of Medicine, Columbia, Missouri 65212, United States

Abstract

Age-related cataract formation is marked by the progressive aggregation of lens proteins. The formation of protein aggregates in the aging lens has been shown to correlate with the progressive accumulation of a range of post-translational crystallin modifications, including oxidation, deamidation, racemization, methylation, acetylation, N- and C-terminal truncations and low molecular weight (LMW) crystallin fragments. We found that an αA-crystallin-derived peptide, αA66-80 (1.8 Kda), is a prominent LMW peptide concentrated in water-insoluble fractions of the aging lens. The peptide has amyloid-like properties and preferentially insolubilizes α-crystallin from lens-soluble fractions. It binds at multiple sites and forms a hydrophobically driven non-covalent complex with α-crystallin to induce α-crystallin aggregation. To define the specific role of the αA66-80 peptide in age-related protein aggregation and cataract formation, it is important to understand the mechanisms by which this peptide acts. We used scanning proline mutagenesis to identify which particular sequences of the peptide drive it to form amyloid-like fibrils and induce α-crystallin aggregation. The secondary structure and the aggregate morphology of the peptides were determined using circular dichroism and transmission electron microscopy, respectively. Peptides were also tested for their ability to induce α-crystallin aggregation. We found that proline replacement of any residue in the sequence FVIFLDV, which corresponds to residues 71-77, led to an absence of both fibril formation and α-crystallin aggregation. The apparently critical role of 71-77 residues in αA66-80 explains their significance in the self-assembly processes of the peptide and further provide insights into the mechanism of peptide-induced aggregation. Our findings may have applications in the design of peptide aggregation inhibitors.

Keywords

crystallin; amyloid fibril; protein aggregation; cataract

*Corresponding author Prof. Krishna Sharma Department of Ophthalmology, EC213, University of Missouri, One Hospital Drive, Columbia, MO 65212. sharmak@health.missouri.edu. Telephone: 1 (573) 882-8478. Fax: 1 (573) 884-4100.

Declaration of interest
The authors report no conflict of interest.

1. Introduction

Cataract is the most common age-related disorder of the eye lens and is associated with the formation of light scattering high molecular weight (HMW) aggregates. These HMW aggregates are composed of primarily modified crystallin proteins and their degradation products [1-7]. There are three types of lens crystallins—α, β and γ—and they are the structural proteins responsible for lens transparency. α-Crystallin is the major soluble protein and constitutes 40% of crystallins. It is made up of two subunits: αA and αB. Native α-crystallins as well as recombinant αA- and αB-crystallins possess chaperone-like activity and prevent the aggregation of partially unfolded substrates. Lens crystallins undergo age-related changes such as deamidation, racemization, methylation,acetylation [8,9], increased crystallin breakdown [10] and progressive accumulation of specific LMW peptides [5, 9], which eventually lead to the formation of HMW protein aggregates [6]. With aging, because the quality control system deteriorates, there is a buildup of crystallin fragments [5,7,10,12]. Aged lenses are known to contain more crystallin fragments than younger lenses [11,12]. A strong correlation observed between the accumulation of crystallin fragments and an increase in the content of water-insoluble proteins in the lens supports the hypothesis that the age-related accumulation of LMW peptides is a triggering or facilitating factor for the aggregation of lens proteins [7].

Among the LMW peptides, the αA-crystallin-derived αA66-80 peptide, with its 15 amino acids, has been found to be the most prevalent LMW peptide in the water-insoluble fractions of lenses[13], with the increase in the appearance of αA66-80 peptide in lenses being age dependent[12,13]. The peptide carries part of the chaperone site [14] and has sequences homologous to Aβ-sequences [15]. Our biophysical characterization studies showed that the peptide has a β-sheet structure and assembles into amyloid-like fibrils *in vitro* [13]. Fibrillations by small peptides have been reported earlier [16-18]. The αA66-80 peptide binds to multiple sites in α-crystallin, including the chaperone site, the subunit interaction region and the C-terminal extension. The αA66-80 peptide suppresses α-crystallin chaperone activity, decreases the solubility of α-crystallin and increases the surface hydrophobicity in α-crystallin by forming stable non-covalent interactions with α-crystallin [19]. In order to understand the mechanisms of peptide-induced aggregation and to design inhibitors to control peptide-mediated protein precipitation, it is important to identify which amino acids in the primary sequence of the peptide are critical for its aggregation activity.

Systematic replacement of the amino acids in a protein or in a peptide sequence with proline has been used extensively to determine the role of each amino acid of a particular peptide [20,21]. In this study we sought to delineate the role of each residue of the 15 amino acid αA66-80 by performing sequential proline scanning of the peptide. We also performed circular dichroism studies to determine the secondary structural features adopted by proline-substituted peptides. We examined the morphological structures of the peptide variants by electron microscopy and compared their structure to that of the amyloid-like fibrils of αA66-80. We found that residues 71-77 and the 79^{th} residue are critical for the peptide's aggregation activity.

2. Materials and methods

2.1 Preparation of peptides

Wild-type (WT) αA66-80 was obtained as a 98% pure peptide from Genscript Corporation (Piscataway, NJ). αA66-80 peptides with proline replacements (>70% purity) were purchased from Sigma-Aldrich, Inc. (St. Louis, MO). Peptides were dissolved in 0.05% trifluoroacetic acid and purified by high-performance liquid chromatography (HPLC) using a C18 reversed-phased column (Vydac). The peptides were purified using a linear gradient of buffer B (0.1% TFA in acetonitrile) and buffer A (0.1% TFA in water), 0-10% B run for 5 min, followed by 10-60% B run over 35 min at a flow rate of 1ml/min. Re-chromatography of the purified peptides by HPLC showed >90% purity. Purified peptides were disaggregated via treatment with 1,1,1,3,3,3,-hexafluoro-2-isopropanol (HFIP), using a modified procedure as described previously [21]. The peptides were dissolved in HFIP (2:1 w/v), vortexed for 10 min and sonicated using the standard probe with 0.125 inch (3 mm) tip set to pulse (Sonic Disembrator, Model 100, Fisher Scientific, Pittsburgh, PA) for 10 min. The peptides were then evaporated in a Savant SpeedVac system (Model SC-100, Thermo Scientific). These HFIP dissolving and evaporation steps were repeated three times. The dried peptides were stored at −80° C before use. Prior to the experiments, the peptides were dissolved in sterile water. The concentration of the peptide was estimated by absorption at 220 nm using a standard curve with 98% pure WT αA66-80 in a dual beam spectrophotometer (UV-2401 PC, Shimadzu).

2.2 Circular dichroism (CD) spectroscopy

Prior to the CD experiments, peptide samples (200 μg /ml) were prepared in 50 mM phosphate buffer, pH 7.2 containing 150 mM NaCl. Far UV CD spectra (190 – 250 nm) were acquired using Jasco J-815 spectrofluorometer in 0.2 cm quartz cells. Spectra were recorded at room temperature and 1 nm resolution with a scan rate of 50 nm/min. An average of five scans was recorded for each sample. Raw data were manipulated by subtraction of appropriate background spectra and expressed as molar ellipticity.

2.3 Transmission electron microscopy

Each αA66-80 peptide derivative (1 mg/ml) was incubated in 50 mM phosphate buffer (pH 7.2) containing 150 mM NaCl for 24 hrs at 37°C. The suspensions were applied to a copper grid and allowed to dry in air before being negatively stained for 2 min with 2% uranyl acetate. Samples were examined with a JEOL JEM-1400 microscope (JEOL Ltd.,Tokyo Japan) at 120kV. Fibril widths were analyzed (n=3 for each sample) using ImageJ software developed by Wayne Rasband, National Institutes of Health, Bethesda, MD,(at http://rsb.info.nih.gov/ij).

2.4 Aggregation of α-crystallin by peptides

α-Crystallin (100 μg) mixed with peptides (50 μg each) was incubated at 37°C for 24 hrs. After incubation, the samples were centrifuged at 8000 rpm for 30 min. Pellets were redissolved in 20 μl of urea (6 M) and diluted to a total volume of 100 μl with 50 mM phosphate buffer (pH 7.2). A 25 μl aliquot of redissolved pellets was combined with 2X

SDS buffer and loaded onto a 4-20% Tris-HCl gel (Pierce), run at 100V and Coomassie stained. Gels were imaged with a Bio-Rad-ChemDoc XRS+imaging system and bands corresponding to α-crystallin were quantified for their intensity using Image lab software (Bio-Rad). Using a standard graph constructed with 2 to 15 μg of α-crystallin bands on the gel, the crystallin aggregate band intensity was converted to α-crystallin protein. The amount of crystallin precipitated by representative peptides (S66P and L75P) was also estimated by measuring the protein concentrations at 280 nm in the supernatant and in the pellet re-dissolved in 6M urea containing buffer.

3. Results

Identifying the critical residues in αA66-80 peptide responsible for its aggregation behavior is a key to understanding the mechanisms of peptide-induced aggregation as well as for designing peptide inhibitors. Proline or alanine scanning offers a promising tool to analyze the characteristic contributions of the residues in a peptide. Secondary structure and conformational characteristics of the Aβ peptide have been studied using similar approaches [21,22]. We used systematic proline scanning of the αA66-80 peptide to identify its critical residues. **Fig 1A** shows the αA66-80 sequence of human αA-crystallin. **Fig 1B** shows the proline substitutions of the peptide that were used in the study.

3.1 Secondary structure of peptides

CD studies were used to evaluate the fundamental β-sheet structure of the αA66-80 peptide and the effect of the proline replacement to inhibit the β-sheet structure. Far-UV CD spectra of the freshly prepared proline-substituted peptides in comparison with WT αA66-80 are presented in **Fig 2 (panels A to P)**. The spectra of WT αA66-80 exhibited a 218nm minimum, typical for β-sheet structure [23]. Except for the peptide with proline replaced at the 68th position, all of the other peptides displayed a secondary structural conformation that varied from the WT αA66-80 peptide. R68P exhibited a β-sheet structural feature similar to that of the WT αA66-80. H79P featured an extended conformation with a positive band around 215 nm and a small negative band around 225 nm. The spectrum of peptides containing proline replacements at 66, 71, 72, 73, 75, 76, 77 and 78 had a minimum near 200 nm as a predominant feature, typical for an unordered or random coil structure [23]. Proline substitutions in these regions thus make a conformation of β-sheet unfavorable..

3.2 Morphology of peptide aggregates

Next, we characterized the aggregate structures formed by the various peptides by transmission electron microscopy (TEM). Peptide solutions (1 mg/ml) were incubated at 37°C for 24 hrs in 50 mM phosphate buffer, pH 7.2. Fibrillar structures were found for some of the peptides, albeit with considerable morphological differences. Fig 2 compares the secondary structure and the aggregate morphology of the peptides. As shown in **Fig 2 (panel A)**, after 24 hrs of incubation, WT αA66-80 formed long, rigid, well-separated and extended fibrils with a width 12 ± 0.5 nm, consistent with the observations made previously [13]. Under the same conditions, peptide with proline replacement at Ser 66 formed short, kinked, curvy and dispersed fibrils (width 7.5 ±0.9 nm) (Fig 2, **panel B**) that associated with each other, but did not assemble into lengthy fibrils. The appearance of fibril-like structures

formed by D67P and D69P peptides was at low frequency compared to WT peptide. Minimal aggregation was noted, with only an occasional, solitary long fibril, a slightly wider fibril in D67P (width, 23 ± 2 nm) and a well-defined long fibril in D69 P (width 15 ±1 nm) (Fig 2 **panels C & E**). The proline mutants at the 70th position assembled into twisted doublet, well-defined fibrils, which are seemingly rigid and wider and have a smooth surface (width 25 ±5 nm) (Fig 2 **panel F**). Prolines at positions 71-77 completely eliminated the fibril-forming capacity of the peptide (Fig 2-**panel G to M**), whereas prolines at positions 66-69 resulted in slightly inhibited fibrilization. Replacement of His79 eliminated fibril formation (Fig 2-**panel O**), even though the replaced residue is only one amino acid away from the C-terminus of the peptide. In contrast, proline replacement of the amino acids Arg 68 and Lys70, which are 2-4 residues from the N-terminus, resulted in good fibril formation (Fig 2-**panel D & F**), suggesting that residues Arg 68 and Lys 70 are not intimately involved in good fibril formation. The fibrils formed by F80P peptide consisted of dense filamentous aggregates intermixed with longer fibrils (width 9.5 ± 1 nm) showing positive and negative staining. The lack of detectable fibrils in peptides with proline replacements at 71-77 is in accordance with the random structure seen in CD (**Fig 2- panel G to M**). Thus, proline replacements at 71-77 bring about changes in the amyloid fibril morphology by modifying or interrupting or destroying the entire segments of the β-extended chain.

3.3 Aggregation of α-crystallin by proline mutants of αA66-80

In order to probe the impact of proline on αA66-80-mediated α-crystallin aggregation, αA66-80 and its proline-substituted derivatives were incubated with α-crystallin at a 2:1 ratio (w/w) for 24 hrs at 37°C. We performed SDS-PAGE on the pellets of samples after centrifugation (**Fig 3A**). The stained gels reveal that α-crystallin was precipitated by the peptides when proline replacements were at S66, D67, R68, D69, K70 and F80. Notably, the highest amount of aggregate occurred in α-crystallin incubated with proline substituted at positions 66 and 67 of the peptides. Aggregation of 53% and 52% of α-crystallin occurred when proline was substituted at positions 66 and 67, respectively. In contrast, aggregation of 34%, 33%, 29%, 25% and 20% of α-crystallin occurred with proline replacement at R68P, K70P, D69P, F80P and K78P respectively. Incubations with F71P, V72P, F74P, L75P, D76P, V77P and H79P resulted in <10% precipitation of –crystallin. After incubation of α-crystallin with representative peptides S66P and L75P, direct measurement (A280 absorption) of the α-crystallin that remained soluble in supernatants showed that 46% and 91% of α-crystallin remained in solution. These values are comparable to the values estimated after SDS-PAGE band intensity analysis (Fig 3B). Crystallin aggregating ability of these peptides, evident from gel electrophoresis, correlated with the propensity exhibited by the peptides in forming fibrils (**Fig 2 &3**). Proline substitution anywhere in the region of residues 71-79 rendered the peptide incapable of aggregating α-crystallin, (**Fig 3 A&B**), with the peptides lacking fibril-forming capacity as well (**Fig 2**). These results suggest that residues 71-79 of αA66-80 are important for inducing and facilitating α-crystallin aggregation.

4 Discussion

The ability of the αA66-80 peptide to induce aggregation of α-crystallin gains significance on account of its increased appearance in the water-insoluble fractions of aging lenses. Using systematic proline replacements, we attempted to identify the critical residue(s) in the peptide that are involved in its β-sheet conformation, its fibril-forming ability and its capacity to induce α-crystallin aggregation. In our CD studies, WT αA66-80 displayed a β-sheet conformation, in agreement with the structural feature of an amyloidogenic sequence. The substitution of WT αA66-80 residues with proline resulted in an alteration in the secondary structure. Except for peptides with proline replacements at D67, R68 and D69, all of the other peptides displayed random conformation. Our CD results reconfirm the fact that prolines are rarely found in β-sheets, as the presence of proline imposes constraints with $\Phi = -60^0$ as opposed to $\Phi = -120^0, \psi = 140^0$ geometries, typical for a peptide bond found in β-sheets [24]. Thus, in agreement with the earlier observations [20], amyloidogenic sequences such as WT αA66-80 peptide are intolerant of proline replacements.

Our transmission electron microscopy studies of proline-substituted αA66-80 peptides incubated for 24 hours showed that proline substitutions give rise to changes in the aggregation propensity and fibril formation. Proline substitutions at N-terminal regions resulted in aggregation and gradual transformation into fibrils. Peptides with substitutions at 66, 67, 68, 69 and 70 positions behaved similarly to WT αA66-80, but exhibited slightly different fibrillar morphology. Proline substitutions at positions 71-77 made β-sheet conformation unfavorable and affected the fibril-forming ability of the αA66-80 peptide. Residues 71-75 (FVIFL) and 77 (V) contain hydrophobic amino acids and are homologous to residues 16-20 (KLVFF) of the Aβ (1-42) peptide [15]. Previous studies with Aβ peptide identified 16-20 (KLVFF) hydrophobic core as critical for aggregation [25,26]. Thus, the lack of fibril-forming ability of the αA66-80 peptides with proline substitutions at 71-77 points to their importance in fibril formation. These proline- substituted peptides also did not bring about aggregation of α-crystallin. The π-stacking of aromatic residues has been observed as a key feature in the amyloid fibril assembly and aggregation [27-29]. Peptide fragments of islet amyloid polypeptide (IAPP) and calcitonin, both associated with amyloid-based diseases, have shown diminished fibril formation when phenylalanines are replaced with alanine [16, 26, 30, 31]. Given these precedents showing the importance of π-stacking in dictating amyloid structure, it is not surprising that F71P and F74P – αA66-80 peptides have significantly impaired ability to form fibrils as well as to aggregate α-crystallin. However, we found that proline replacement at F80 does not affect fibril formation. F71 and F74 are part of the hydrophobic stretch that forms the core, whereas F80 is at the C-terminus. Our results suggest that the aggregation propensity of the αA66-80 peptide is primarily due to hydrophobic packing, with π-stacking interactions also playing a role.

The results of our systematic proline scanning studies suggest the presence of a specific molecular recognition involving the central hydrophobic residues (residues 71-75) seems to be the absolute key in determining the aggregation tendency of α-crystallin. These findings correlate with the previous observation that hydrophobic interactions stabilize αA66-80–α-crystallin complexes and that the peptide increases the surface hydrophobicity of α-crystallin, which in turn drives the aggregation process [19].

Acknowledgments

This work was supported by National Institutes of Health Grant EY019878 and an unrestricted grant-in-aid from Research to Prevent Blindness to the Department of Ophthalmology. We thank Sharon Morey for her help in editorial work.

Abbreviations

HMW	high molecular weight
LMW	low molecular weight
CD	circular dichroism
SDS-PAGE	sodium dodecyl sulfate- Polyacrylamide gel electrophoresis

References

1. Horwitz J, Hansen JS, Cheung CC, Ding LL, Straatsma BR, Lightfoot DO, Takemoto LJ. Presence of low molecular weight polypeptides in human brunescent cataracts. Biochem Biophys Res Commun. 1983; 113:65–71. [PubMed: 6860343]
2. Harrington V, McCall S, Huynh S, Srivastava K, Srivastava OP. Crystallins in water soluble-high molecular weight protein fractions and water insoluble protein fractions in aging and cataractous human lenses. Mol Vis. 2004; 10:476–489. [PubMed: 15303090]
3. Harrington V, Srivastava OP, Kirk M. Proteomic analysis of water insoluble proteins from normal and cataractous human lenses. Mol Vis. 2007; 13:1680–1694. [PubMed: 17893670]
4. Srivastava K, Chaves JM, Srivastava OP, Kirk M. Multi-crystallin complexes exist in the water-soluble high molecular weight protein fractions of aging normal and cataractous human lenses. Exp Eye Res. 2008; 87:356–366. [PubMed: 18662688]
5. Sharma KK, Santhoshkumar P. Lens aging: effects of crystallins. Biochim Biophys Acta. 2009; 1790:1095–1108. [PubMed: 19463898]
6. Bloemendal H, de Jong W, Jaenicke R, Lubsen NH, Slingsby C, Tardieu A. Ageing and vision: structure, stability and function of lens crystallins. Prog Biophys Mol Biol. 2004; 86:407–485. [PubMed: 15302206]
7. Santhoshkumar P, Udupa P, Murugesan R, Sharma KK. Significance of interactions of low molecular weight crystallin fragments in lens aging and cataract formation. J Biol Chem. 2008; 283:8477–8485. [PubMed: 18227073]
8. Jaisson S, Gillery P. Evaluation of nonenzymatic posttranslational modification-derived products as biomarkers of molecular aging of proteins. Clin Chem. 2010; 56:1401–1412. [PubMed: 20562349]
9. Truscott RJ. Macromolecular deterioration as the ultimate constraint on human lifespan. Ageing Res Rev. 2011; 10:397–403. [PubMed: 21272671]
10. Srivastava OP. Age-related increase in concentration and aggregation of degraded polypeptides in human lenses. Exp Eye Res. 1988; 47:525–543. [PubMed: 3181333]
11. Michael R, Bron AJ. The ageing lens and cataract: a model of normal and pathological ageing. Philos Trans R Soc Lond B Biol Sci. 2011; 366:1278–1292. [PubMed: 21402586]
12. Su SP, McArthur JD, Andrew Aquilina J. Localization of low molecular weight crystallin peptides in the aging human lens using a MALDI mass spectrometry imaging approach. Exp Eye Res. 2010; 91:97–103. [PubMed: 20433829]
13. Santhoshkumar P, Raju M, Sharma KK. AlphaA-crystallin peptide SDRDKFVIFLDVKHF accumulating in aging lens impairs the function of alpha-crystallin and induces lens protein aggregation. PLoS One. 2011; 6:0019291.
14. Sharma KK, Kumar RS, Kumar GS, Quinn PT. Synthesis and characterization of a peptide identified as a functional element in alphaA-crystallin. J Biol Chem. 2000; 275:3767–3771. [PubMed: 10660525]

15. Santhoshkumar P, Sharma KK. Inhibition of amyloid fibrillogenesis and toxicity by a peptide chaperone. Mol Cell Biochem. 2004; 267:147–155. [PubMed: 15663196]
16. Westermark P, Engström U, Johnson KH, Westermark GT, Betsholtz C. Islet amyloid polypeptide: pinpointing amino acid residues linked to amyloid fibril formation. Proc Natl Acad Sci. 1990; 87:5036–5040. [PubMed: 2195544]
17. Nguyen HD, Hall CK. Kinetics of fibril formation by polyalanine peptides. J Biol Chem. 2005; 280:9074–9082. [PubMed: 15591317]
18. Srinivasan R, Jones EM, Liu K, Ghiso J, Marchant RE, Zagorski MG. pH-dependent amyloid and protofibril formation by the ABri peptide of familial British dementia. J Mol Biol. 2003; 333:1003–1023. [PubMed: 14583196]
19. Kannan R, Santhoshkumar P, Mooney BP, Sharma KK. The alphaA66-80 Peptide Interacts with Soluble alpha-Crystallin and Induces Its Aggregation and Precipitation: A Contribution to Age-Related Cataract Formation. Biochemistry. 2013; 16:16.
20. Wood SJ, Wetzel R, Martin JD, Hurle MR. Prolines and amyloidogenicity in fragments of the Alzheimer's peptide beta/A4. Biochemistry. 1995; 34:724–730. [PubMed: 7827029]
21. Williams AD, Portelius E, Kheterpal I, Guo JT, Cook KD, Xu Y, Wetzel R. Mapping abeta amyloid fibril secondary structure using scanning proline mutagenesis. J Mol Biol. 2004; 335:833–842. [PubMed: 14687578]
22. Morimoto A, Irie K, Murakami K, Masuda Y, Ohigashi H, Nagao M, Fukuda H, et al. Analysis of the secondary structure of beta-amyloid (Abeta42) fibrils by systematic proline replacement. J Biol Chem. 2004; 279:52781–52788. [PubMed: 15459202]
23. Yang JT, Wu CS, Martinez HM. Calculation of protein conformation from circular dichroism. Methods Enzymol. 1986; 130:208–269. [PubMed: 3773734]
24. Chou PY, Fasman GD. Conformational parameters for amino acids in helical, beta-sheet, and random coil regions calculated from proteins. Biochemistry. 1974; 13:211–222. [PubMed: 4358939]
25. Esler WP, Stimson ER, Ghilardi JR, Lu YA, Felix AM, Vinters HV, Mantyh PW, et al. Point substitution in the central hydrophobic cluster of a human beta-amyloid congener disrupts peptide folding and abolishes plaque competence. Biochemistry. 1996; 35:13914–13921. [PubMed: 8909288]
26. Hilbich C, Kisters-Woike B, Reed J, Masters CL, Beyreuther K. Substitutions of hydrophobic amino acids reduce the amyloidogenicity of Alzheimer's disease beta A4 peptides. J Mol Biol. 1992; 228:460–473. [PubMed: 1453457]
27. Adler-Abramovich L, Vaks L, Carny O, Trudler D, Magno A, Caflisch A, Frenkel D, et al. Phenylalanine assembly into toxic fibrils suggests amyloid etiology in phenylketonuria. Nat Chem Biol. 2012; 8:701–706. [PubMed: 22706200]
28. Gazit E. A possible role for pi-stacking in the self-assembly of amyloid fibrils. Faseb J. 2002; 16:77–83. [PubMed: 11772939]
29. Gazit E. Self assembly of short aromatic peptides into amyloid fibrils and related nanostructures. Prion. 2007; 1:32–35. [PubMed: 19164892]
30. Reches M, Porat Y, Gazit E. Amyloid fibril formation by pentapeptide and tetrapeptide fragments of human calcitonin. J Biol Chem. 2002; 277:35475–35480. [PubMed: 12095997]
31. Azriel R, Gazit E. Analysis of the minimal amyloid-forming fragment of the islet amyloid polypeptide. An experimental support for the key role of the phenylalanine residue in amyloid formation. J Biol Chem. 2001; 276:34156–34161. [PubMed: 11445568]

A

66 – SDRDKFVIFLDVKHF -80

Red: acidic residues; Blue: basic residues

Green: hydrophobic uncharged residues; Black: other residues

B

αA66-80	NH_2 – SDRDKFVIFLDVKHF –COOH
S66P	NH_2 – PDRDKFVIFLDVKHF –COOH
D67P	NH_2 – SPRDKFVIFLDVKHF –COOH
R68P	NH_2 – SDPDKFVIFLDVKHF –COOH
D69P	NH_2 – SDRPKFVIFLDVKHF –COOH
K70P	NH_2 – SDRDPFVIFLDVKHF –COOH
F71P	NH_2 – SDRDKPVIFLDVKHF –COOH
V72P	NH_2 – SDRDKFPIFLDVKHF –COOH
I73P	NH_2 – SDRDKFVPFLDVKHF –COOH
F74P	NH_2 – SDRDKFVIPLDVKHF –COOH
L75P	NH_2 – SDRDKFVIFPDVKHF –COOH
D76P	NH_2 – SDRDKFVIFLPVKHF –COOH
V77P	NH_2 – SDRDKFVIFLDPKHF –COOH
K78P	NH_2 – SDRDKFVIFLDVPHF –COOH
H79P	NH_2 – SDRDKFVIFLDVKPF –COOH
F80P	NH_2 – SDRDKFVIFLDVKHP –COOH

Figure 1.

A. Amino acid sequence of αA66-80 peptide. Residues in color denote the charge attribute.

B. The designations and sequences of the proline-substituted αA66-80 peptides used in the study.

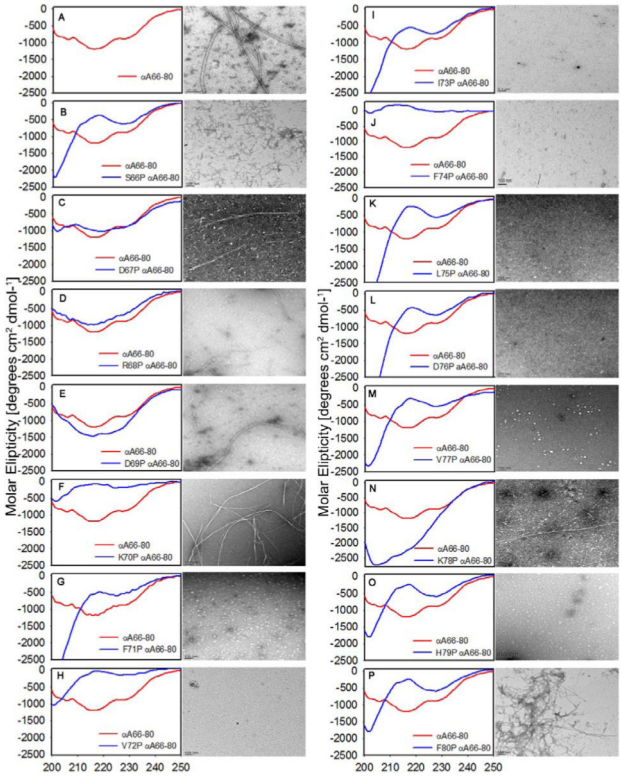

Figure 2.

Far-UV CD spectra (left) and aggregate morphology (right) of peptides - **(A)** WT αA 66-80, scale bar 100nm; **(B)** S66P, **(C)** D67P **(D)** R68P,**(E)**D69P**,(F)** K70P **,(G)** F71P, **(H)** V72P **(I)** I73P, **(J)** F74P, **(K)** L75P and **(L)** D76P **(M)** V77P, **(N)** K78P, **(O)** H79P and **(P)** F80P, (scale bar 100 nm). CD spectra were acquired for freshly prepared peptides (200μg each) in 50mM phosphate buffer (pH 7.2). A 1mg/ml preparation of peptides incubated for 24 hrs at 37°C in 50mM phosphate buffer (pH 7.2) were examined by TEM.

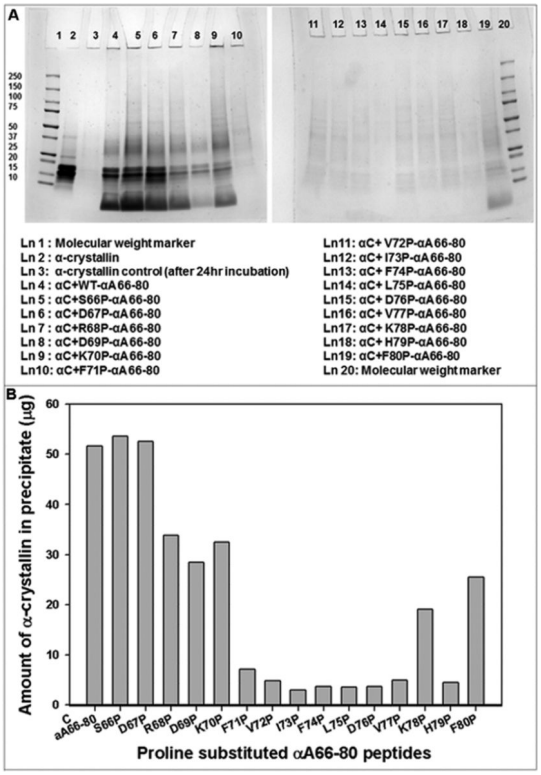

Figure 3.

A. SDS-PAGE of redissolved pellets of α-crystallin (αC) samples incubated with WT αA66-80 and proline-substituted αA66-80 peptides. α-Crystallin (100 µg) and peptides (each 50 µg) in 500 µl of 50 mM phosphate buffer (pH 7.2) were incubated for 24 hrs at 37°C. After incubation, samples were centrifuged at 8000 rpm for 30 min. Pellets were redissolved in 20 µl of urea (6 M) and diluted to a total volume of 100 µl with 50 mM phosphate buffer (pH 7.2). A 25 µl aliquot of each sample was mixed with sample buffer and run in 4-20% SDS-PAGE. Lane 3 shows pellet formed after 24 hr incubation of α-crystallin by itself. Lane 4 to lane 19 represents the pellets formed after 24 hr incubation of α-crystallin with peptides. **B.** Aggregation of α-crystallin in the presence of proline-substituted αA66-80 peptides. The intensity of SDS-PAGE protein bands from figure 3 A were quantified using Image Lab Software (Bio-Rad). The band intensity values are converted to microgram based on standard graph constructed with band intensity for 2-15 µg of α-crystallin.